Development 125, 753-765 (1998)
Printed in Great Britain © The Company of Biologists Limited 1998
DEV4961

Fibroblast growth factor receptor 2 (FGFR2)-mediated reciprocal regulation loop between FGF8 and FGF10 is essential for limb induction

Xiaoling Xu[1], Michael Weinstein[1], Cuiling Li[1], Michael Naski[3], Rick I. Cohen[2], David M. Ornitz[3], Philip Leder[4] and Chuxia Deng[1,*]

[1]Laboratory of Biochemistry and Metabolism, National Institute of Diabetes, Digestive and Kidney Diseases, 10/9N105, and
[2]Laboratory of Developmental Neurogenetics, National Institutes of Health, Bethesda, MD 20892, USA
[3]Department of Molecular Biology and Pharmacology, Washington University Medical School, 660 S. Euclid Avenue, St. Louis, MO 63110, USA
[4]Department of Genetics, Harvard Medical School, Howard Hughes Medical Institute, 200 Longwood Avenue, Boston, MA 02115, USA
*Author for correspondence (e-mail: ChuxiaD@BDG10.NIDDK.NIH.Gov)

Accepted 25 November 1997: published on WWW 22 January 1998

SUMMARY

FGFR2 is a membrane-spanning tyrosine kinase that serves as a high affinity receptor for several members of the fibroblast growth factor (FGF) family. To explore functions of FGF/FGFR2 signals in development, we have mutated FGFR2 by deleting the entire immunoglobin-like domain III of the receptor. We showed that murine FGFR2 is essential for chorioallantoic fusion and placenta trophoblast cell proliferation. *Fgfr2*$^{\Delta IgIII/\Delta IgIII}$ embryos displayed two distinct defects that resulted in failures in formation of a functional placenta. About one third of the mutants failed to form the chorioallantoic fusion junction and the remaining mutants did not have the labyrinthine portion of the placenta. Consequently, all mutants died at 10-11 days of gestation. Interestingly, *Fgfr2*$^{\Delta IgIII/\Delta IgIII}$ embryos do not form limb buds. Consistent with this defect, the expression of *Fgf8*, an apical ectodermal factor, is absent in the mutant presumptive limb ectoderm, and the expression of *Fgf10*, a mesenchymally expressed limb bud initiator, is down regulated in the underlying mesoderm. These findings provide direct genetic evidence that FGF/FGFR2 signals are absolutely required for vertebrate limb induction and that an FGFR2 signal is essential for the reciprocal regulation loop between FGF8 and FGF10 during limb induction.

Key words: FGFR2, Chorioallantoic fusion, Placentation, FGF8 induction, *Fgf10* expression, Limb bud initiation

INTRODUCTION

The vertebrate limb bud is an excellent model for studying developmentally related signals (reviewed by Tabin, 1995). The limb bud is initiated by the continued proliferation of cells of the lateral plate mesoderm at the axial levels between the 8-12th somites in mouse. Signals from the rapidly proliferating mesodermal cells induce the ectoderm at the tip of the limb bud to form a specialized structure called the apical ectodermal ridge (AER). Once induced, the AER becomes essential for the sustained outgrowth and the pattern formation of the limb through interactions with the underlying mesenchyme (Laufer et al., 1994; Niswander et al., 1994, 1993).

Fibroblast growth factors (FGFs), which constitute a gene family of at least 15 members (Smallwood et al., 1996; Verdier et al., 1997; Yamasaki et al., 1996; McWhirter et al., 1997) are essential signaling molecules for mesenchymal-ectodermal interactions during limb development. *In situ* hybridization studies showed that several FGFs are expressed during limb bud initiation and in the AER (Heikinheimo et al., 1994; Savage and Fallon 1995; Crossley and Martin 1995; Mahmood et al., 1995; Crossley et al., 1996; Ohuchi et al., 1997; Vogel et al., 1996). It was shown that FGF4 (Niswander and Martin, 1993; Niswander et al., 1993) or FGF2 (Fallon et al., 1994) can substitute for AER signals and promote virtually complete outgrowth and patterning of the chick limb. Remarkably, it was also demonstrated that FGF-soaked beads were capable of inducing the formation of complete, morphologically normal limb buds when implanted in the presumptive flank of chick embryos (Cohn et al., 1995; Crossley et al., 1996; Ohuchi et al., 1997). Together, these studies suggest that FGF signals are essential for the initiation, growth and patterning of embryonic limbs.

FGF signals are mediated by a group of four transmembrane proteins with intrinsic tyrosine kinase activity, known as FGF receptors (FGFRs) (Basilico and Moscatelli, 1992; Johnson and Williams, 1993). These receptors share several common structural features, including a hydrophobic leader sequence, three immunoglobulin (Ig) like domains, an acidic box, a CAM (cell adhesion molecule) homology domain, a transmembrane

region, and a divided tyrosine kinase domain. Numerous mRNA isoforms of the *Fgf* receptor genes are generated by alternative splicing in the extracellular, juxtamembrane, and intracellular domains (reviewed by Givol and Yayon, 1992). RNA in situ hybridization studies showed that FGFRs are expressed in a variety of tissues and organs throughout vertebrate development with a distinct expression pattern for each receptor. Generally, *Fgfr1* is expressed almost exclusively in mesenchyme (Orr-Urtreger et al., 1991; Peters et al., 1992; Yamaguchi et al., 1992). *Fgfr2* is predominantly in epithelium (Orr-Urtreger et al., 1993, 1991; Peters et al., 1992). *Fgfr3* is expressed in the developing central nervous system as well as in bone rudiments (Peters et al., 1993), and *Fgfr4* is expressed in the definitive endoderm and the somatic myotome (Stark et al., 1991). This expression pattern suggests that each receptor may play an important, yet distinct, role during vertebrate development.

Much of our understanding of the functions of FGF receptors in development comes from mutational analyses of the receptor in a number of organisms. FGF receptor mutations have been linked to migration failures of sex myoblasts in *C. elegans* (DeVore et al., 1995) and tracheal cells in *Drosophila* (Beiman et al., 1996; Gisselbrecht et al., 1996; Reichman-Fried et al., 1994; Reichman-Fried and Shilo, 1995). In *Xenopus*, expression of a dominant-negative (dn) FGFR construct inhibits the formation of ventral and posterior mesoderm (Amaya et al., 1991). Similarly, dn FGF receptors targeted to mouse lung or skin were reported to completely block the branching morphogenesis of the lung (Peters et al., 1994) and disrupted the organization of epidermal keratinocytes (Werner et al., 1993), respectively. Using targeted gene disruption, we and others found that *Fgfr1* is essential for early embryonic growth and mesoderm patterning (Deng et al., 1994; Yamaguchi et al., 1994). Further study of chimeric mouse embryos formed using FGFR1 null ES cells revealed a role of FGFR1 in multiple developmental processes, including posterior neural tube development, and the growth and pattering of the limb buds (Ciruna, 1997; Deng et al., 1997).

Involvement of FGFs in skeletal development was revealed recently by the mapping of at least eight human skeletal disorders to FGF receptors 1, 2 and 3 (reviewed by Muenke and Schell, 1995; Mulvihill, 1995). Significantly, all of these disorders are dominant, with craniofacial, appendicular, and/or axial bone abnormalities resulting from point mutations in the FGF receptors. We and others have previously shown that mouse strains which lack either one or both alleles of FGFR1 or FGFR3 do not exhibit any phenotypes that resemble these human disorders (Colvin et al., 1996; Deng et al., 1996, 1994; Yamaguchi et al., 1994). These observations provide compelling evidence that these diseases are not caused by haploinsufficiency or loss-of-function mutations. Interestingly, loss of FGFR3 results in an enhanced chondrogenesis and longer bones, leading to a conclusion that FGFR3 is a negative regulator of bone growth (Colvin et al., 1996; Deng et al., 1996). In our continuous effort to study functions of each FGF receptor in development, and to gain an insight into the mechanism of *Fgfr2* related diseases, we have created mice that carry a targeted deletion of the entire 3rd immunoglobulin-like (Ig) domain of FGFR2 through homologous recombination (Capecchi, 1989). Analysis of the resulting mice indicates that the Ig domain III of FGFR2 is critical for FGF binding and for normal FGFR2 activity. Embryos that lack this domain die at E10-11.5 owing to a failure in chorioallantoic fusion or placental formation. We also show that the deletion of Ig domain III of FGFR2 blocks limb bud initiation. This finding establishes FGFR2 as the major receptor that mediates FGF signals during limb induction.

MATERIALS AND METHODS

Targeting vector

Recombinant phages containing genomic DNA of the *Fgfr2* locus were isolated from a 129 mouse library (Stratagene). To construct the targeting vector for *Fgfr2*, a 3.5 kb *Eco*RV-*Bam*HI fragment that is 3′ to the second exon of the *Fgfr2* gene was subcloned into *Xba*I and *Bam*HI sites of pPNT (Tybulewicz et al., 1991). The resulting construct was cleaved with *Xho*I and *Not*I, followed by insertion of a 6.5 kb *Bam*HI-*Not*I fragment (the *Not*I site is from the polylinker of the phage vector). The finished construct, *pFGFR2neo*, is shown in Fig. 1A.

Homologous recombination in ES cells and generation of germline chimeras

TC1 (Deng et al., 1996) and J1 (Li et al., 1992) ES cells were transfected with *Not*I digested *pFGFR2neo* and selected with G418 and FIAU. The culture, electroporation, and selection of ES cells were carried out as described by Deng et al. (1994). ES cell colonies that were resistant to both G418 and FIAU were analyzed by Southern blotting for homologous recombination events within the *Fgfr2* locus. Genomic DNAs from these clones and the parental TC1 cell line were digested with *Eco*RI, or *Bam*HI, and then probed with a 3′ fragment specific to the *Fgfr2* sequence (Fig. 1B). The 3′ fragment is a PCR product of about 450 bp in length and obtained using the following primer pairs: 5’CTTTAACCTTGAGCTTG3′ and 5′AGAATTTCTAGGGTTG3′. DNAs were also digested using *Bgl*II or *Bam*HI and probed with a probe specific to *neo* gene. The targeted event gives a single band about 20 kb or 11 kb respectively whereas random events give bands of unpredicted sizes.

ES cells heterozygous for the targeted mutation were microinjected into C57BL/6 blastocysts to obtain germline transmission. The injected blastocysts were implanted into the uteri of pseudopregnant Swiss Webster (Taconic) foster mothers and allowed to develop to term. Male chimeras (identified by the presence of agouti coat color) were mated with NIH Black Swiss females (Taconic). Germline transmission was confirmed by agouti coat color in the F_1 animals, and all agouti offspring were tested for the presence of the *Fgfr2* allele by Southern analysis or PCR.

Genotype analysis

For PCR analysis, the wild-type *Fgfr2* allele was detected by using a 5′ oligonucleotide (5′GGTTTACAGCGATCGCCA3′) and a 3′ oligonucleotide (5′GACCTTGAGGTAGGGCAGC3′). This primer pair flanks the *PGKneo* insertion site, and amplifies a 100 bp fragment from the wild-type *Fgfr2* gene. DNA was also amplified using *neo* primers to detect the *neo* gene in the *Fgfr2* allele as described previously (Deng et al., 1994). In this case, a 431 bp fragment is detected in mice heterozygous or homozygous for the *Fgfr2* allele, while no signal can be detected in wild-type mice.

Northern blots

RNA was isolated from E10.5 FGFR2 mutant and normal littermate embryos using RNA Stat-60 based on the protocol suggested by the manufacturer (Tel-Test ‘B,’ Inc.). Poly(A)$^+$ RNA was prepared using

a kit purchased from Pharmacia. About 2 μg of poly(A)$^+$ RNA from each sample was electrophoresed on a 1% agarose gel and transferred to a Gene-Screen filter. The filter was then hybridized with a *Fgfr2* probe as described by Deng et al. (1996).

Histology and antibody staining

To carry out histological studies, embryos were fixed in 4% paraformaldehyde or Bouin's fixative (Sigma) at 4°C overnight, dehydrated through a graded alcohol series, and then embedded in paraffin. Sections of 6-8 μm were prepared and stained with Harris hematoxylin and eosin according to standard procedures. Antibodies to PCNA (PC 10) and FGFR2 were purchased from Signet and Santa Cruz, respectively. The detection was carried out as recommended by the manufacturers.

Scanning electronic microscopy

Embryos were fixed and stored in Tousimis-Johnson Fix (Tousimis) at 4°C. After postfixation in 1% osmium in graded ethanol, the embryos were dried by critical point-drying, mounted on metal studs, coated with gold particles and observed using a scanning electron microscope.

Whole-mount in situ hybridization

Whole-mount in situ hybridization was carried out as described by Riddle et al. (1993). The probes used for the whole-mount in situ hybridization studies were as follows: *Fgfr2* (Deng et al., 1996); *Fgf8* (a full length cDNA that detects all isoforms, Heikinheimo et al., 1994); *Mox-1* (Candia et al., 1992); *Shh* (Chiang et al., 1996); *pl-1, 4311* and *Mash-2* (Guillemot et al., 1994). Mouse *Fgf10* probe is a 543 bp fragment from the 5′UTR of *Fgf10* (A. Blunt; R. Duan and D. M. O., unpublished data).

Construction of soluble FGFR2 binding proteins fused to human placental alkaline phosphatase (AP)

RNAs isolated from E10.5 wild-type and mutant embryos were used as templates for RT-PCR amplification of the extracellular domains of the *Fgfr2* gene, respectively. The primer pair used were a 5′ oligonucleotide: 5′gaagctTGGAGATATGGAAGAGGACC3′ (located in exon 2 before the starting codon) and a 3′ oligonucleotide: 5′ggaagatcTCTCCAGATAATCTGGGGAAG3′ (located in exon 10 prior to the transmembrane portion). The lower case letters are added sequences containing restriction sites. A 1155 bp fragment containing exon 9 (Bek isoform) and a 816 bp fragment (lacking the Ig domain III) were amplified from wild-type and mutant embryos respectively. The PCR products were cut with *Hin*dIII and *Bgl*II, and then subcloned into a *Hin*dIII and *Bgl*II double digested AP expression plasmid (Chellaiah et al., 1994) to generate pFgfr2$^{+/+}$AP and pFgfr2$^{\Delta IgIII/\Delta IgIII}$ AP respectively. The expression vectors were connected at a sequence of *Fgfr2* (5′-3′) and AP (5′-3′). The fusion junctions of both vectors were sequenced and found to be in frame.

AP assay and FGF binding

COS-7 cells were transfected by a standard DEAE-dextran method with 4 μg of plasmid/10^6 cells. Conditioned medium was harvested 3, 6 and 9 days after transfection and used for AP enzyme activity and to determine the relative concentration of the soluble receptors. Binding of the receptor to an immobilized heparin-FGF complex was done as previously described (Gray et al., 1995). Briefly, 10μl bed volume heparin-sepharose was mixed 1:1 with sepharose CL6B and 100 ng FGF2, FGF4 or FGF8. After adding PBS to 50 μl, the mixtures were rotated at room temperature for 1 hour, then washed twice with 100 μl PBS before the addition of receptor supernatant (800 mOD/minute). Following the addition of receptor supernatant, the mixtures were further incubated at room temperature for 4 hours, then washed three times with 200 μl 20 mM Hepes pH 7.5, 150 mM NaCl, 1% Triton X-100, 10% glycerol, and twice with 150 μl 10 mM Tris pH 7.5, 0.5 M NaCl. The receptor-FGF-heparin sepharose complex was transferred in 60 μl 10 mM Tris pH 7.5, to a well of a microtiter plate containing 60 μl of 2× AP assay buffer (2 M diethanolamine, 1 mM $MgCl_2$, 20 mM homoarginine, 12 mM p-nitrophenyl phosphate pH 9.5). The bound receptor was quantified by measuring the initial rate of substrate hydrolysis at 405 nm and same amount of proteins was used in the binding assays.

RESULTS

Targeted deletion of Ig domain III of FGFR2

The targeting construct pFGFR2*neo* (Fig. 1A) was used to delete exons 7, 8 and 9 of the *Fgfr2* gene (Yayon et al., 1992). The linearized pFGFR2*neo* was electroporated into J1 and TC1 ES cells to obtain homologous recombination. Of 339 G418/FIAU double-resistant ES clones from J1 (260 clones) and TC1 (79 clones) cells screened, 3 correct targeting events were identified (2 from J1 and 1 from TC1). The ES cells of all 3 clones were injected into C57BL/6J blastocysts and germline transmission was obtained from the TC1 ES clone. Southern blotting (or PCR amplification of the *neo*^{r} gene) indicated that about 50% of agouti offspring were heterozygous for the introduced mutation (not shown). *Fgfr2*$^{\Delta IgIII/+}$ mice were developmentally normal. Examination of the craniofacial region, skull and limb of these mice did not reveal any abnormalities that resemble the craniosynostosis and limb anomalies commonly seen in Crouzon syndrome (CS), Apert syndrome (AP), Pfeiffer syndrome (PS), Jackson-Weiss syndrome (JW), and the Beare-Stevenson cutis gyrata syndrome (BSCGS) (Przylepa et al., 1996), all diseases that are caused by FGFR2 mutations in humans (reviewed by Muenke and Schell, 1995; Mulvihill, 1995).

Fgfr2$^{\Delta IgIII/\Delta IgIII}$ embryos die at E10.5-11.5

To study the possible effect of the introduced mutation, *Fgfr2*$^{\Delta IgIII/+}$ mice were intercrossed to generate homozygous mice. Of 150 3- to 4-week old mice genotyped, wild-type and *Fgfr2*$^{\Delta IgIII/+}$ mice were detected at a 1:2 ratio, while no homozygotes were found. This observation indicated that the targeted mutation resulted in a recessive embryonic lethal. To determine the timing of *Fgfr2* homozygous lethality, embryos from heterozygous intercrosses at different gestational days were analyzed. As summarized in Table 1, 73 out of 108 decidua isolated from E12.5 to E14.5 contained morphologically normal embryos, while the remaining 35 decidua were much smaller and contained nearly or completely resorbed embryos. Resorptions could not be reliably genotyped because they contained no embryonic material that could be dissected free of maternal tissue. No homozygotes were found among the living embryos. In contrast, at E9.5-10.5, embryos with all three possible genotypes were detected by PCR analysis at a ratio of roughly 1:2:1. All E10.5 homozygous embryos were smaller and were abnormal with respect to limb bud and placenta formation in two different genetic backgrounds (Table 1). PCR genotyping was confirmed by Southern blot analysis which showed that all abnormal embryos analyzed were homozygous for the targeted deletion (Fig. 1B). At E11.5, all embryos homozygous for the targeted mutation were dead and partially resorbed (Table 1). These data indicate *Fgfr2*$^{\Delta IgIII/\Delta IgIII}$ embryos died at E10-11.5 with multiple defects.

Expression of the mutant allele in *Fgfr2*$^{\Delta IgIII/\Delta IgIII}$ embryos

Exons 7, 8 and 9 encode Ig domain IIIa, b and c of FGFR2 (Givol and Yayon, 1992; Yayon et al., 1992). Exons 8 (K) and 9 (B) normally undergo alternative splicing such that the Ig domain III of FGFR2 consists of either IgIIIa/IgIIIb or IgIIIa/IgIIIc which constitutes the KGFR (FGFR2b) or Bek (FGFR2c) isoform, respectively (Fig. 1C). RT-PCR analysis using primer pairs located in exons 6 and 10 revealed a fragment of 218 bp in *Fgfr2*$^{\Delta IgIII/\Delta IgIII}$ and 550 bp in wild-type embryos. Sequencing of these fragments indicated that the 218 bp product was generated by direct splicing from exon 6 to exon 10 (Fig. 1C, Aberrant), and the 550 bp band was composed of two fragments of 554 bp and 557 bp. The 554 bp fragment connects exons 6, 7, 9 and 10 (Fig. 1C, BEK isoform), and the 557 bp fragment connects exons 6, 7, 8 and 10 (Fig. 1C, KGFR isoform). These data indicated that we have deleted 336 bp (exons 7 and 9) from BEK and 339 bp (exons 7 and 8) from KGFR in our mutant embryos. Northern blot analysis of RNA isolated from E10.5 mutant and wild-type embryos indicated that the mutant RNA was transcribed at about one fifth of the normal level (Fig. 1D). Western blot analysis using an anti peptide antibody to the carboxyl end of FGFR2 detected a number of bands of different molecular weights in wild-type embryos. These likely represent both the products of alternative splicing and differential posttranslational modification. However, the most prominent band, which had a relative molecular mass of approximately 125×10^3 and probably represents the full length FGFR2, was completely absent, and the intensity of the 110×10^3 band became significantly weaker in the *Fgfr2*$^{\Delta IgIII/\Delta IgIII}$ embryos (Fig. 1E). To determine if the mutant receptor could still bind to FGF ligands, the extracellular portions of cDNAs from both E10.5 *Fgfr2*$^{\Delta IgIII/\Delta IgIII}$ and wild-type embryos were amplified by PCR, subcloned and subjected to FGF binding analysis. Examination of FGF2, FGF4 and FGF8 indicated that the mutant protein without Ig domain III does not bind to these ligands (Fig. 2).

Absence of chorioallantoic fusion in *Fgfr2*$^{\Delta IgIII/\Delta IgIII}$ embryos

The earliest morphologically visible defect of *Fgfr2*$^{\Delta IgIII/\Delta IgIII}$ embryos was a failure of the allantois to fuse with the chorion. In normal embryos, the allantois and chorion begin to fuse at approximately E8.5-8.75 to form the chorioallantois. However, about one third of the *Fgfr2*$^{\Delta IgIII/\Delta IgIII}$ embryos showed an abnormally enlarged allantois that did not fuse with the chorion. The unfused allantois existed either as a vascular hydropic cyst (Fig. 3A) or as a solid mass (Fig. 3B) of varying shapes. The failure of the chorioallantoic fusion apparently does not have a significant affect on embryonic growth at E8.5-E9 since the

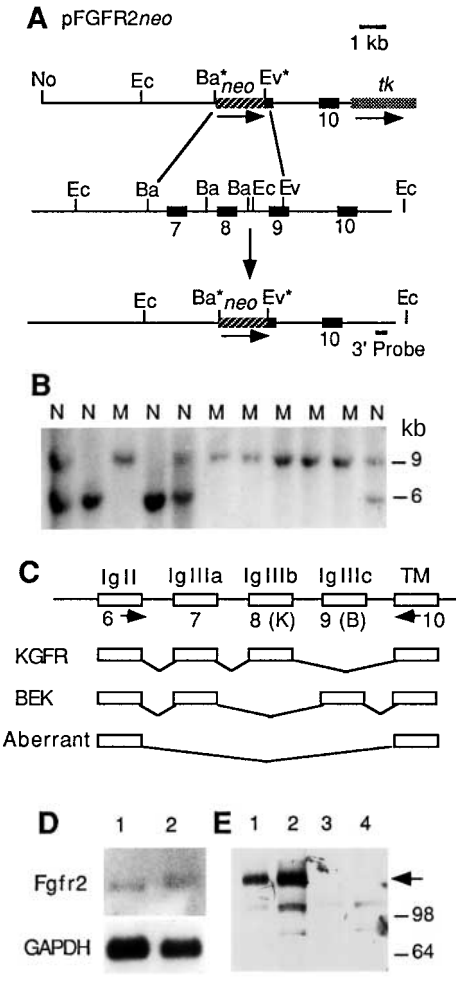

Fig. 1. Targeted deletion of the Ig domain III of the *Fgfr2* gene. (A) Targeting vector pFGFR*2neo* contains a 9 kb *Fgfr2* genomic sequence based on published information (Yayon et al., 1992). The *Fgfr2* sequences are interrupted by *PGKneo* and flanked by a *PGKtk* gene. Homologous recombination within *Fgfr2* would delete a 3.5 kb *Bam*HI-*Eco*RV fragment containing exon 7, 8 and a major portion of exon 9. Ba, *Bam*HI; Ec, *Eco*RI; Ev, *Eco*RV; No, *Not*I. Ba* and Ev* indicated that these two sites were blocked during cloning. (B) Southern blot analysis of DNAs isolated from six abnormal E9.5 embryos generated by intercrosses between *Fgfr2*$^{\Delta IgIII/+}$ mice. Five normal littermates were also included in the blot. DNAs were digested by *Eco*RI and hybridized with the ^{32}P-labeled 3′ flanking probe. The wild-type (6 kb) and mutant (9 kb) fragments were as indicated. All abnormal embryos (M) were *Fgfr2*$^{\Delta IgIII/\Delta IgIII}$ embryos and the normal embryos (N) were either wild type or *Fgfr2*$^{\Delta IgIII/+}$. (C) Alternative splicing around exons 8 or 9 generates KGFR (FGFR2b) or BEK (FGFR2c) isoform in wild-type embryos. However, in FGFR2 mutant embryos, an aberrant splicing form that directly connects exon 6 to exon 10 was detected. Arrows represent primers that were used in RT-PCR. Exon 6 primer: 5′CAAAGGCAACTACACCTGC3′. Exon 10 primer: 5′GAAGTCTGGCTTCTTGGTTCG3′. (D) Northern blot analysis of RNA isolated from E10.5 mutant (lane 1) and wild-type (lane 2) embryos. The full length transcript of *Fgfr2* is about 4.3 kb, while the mutant RNA ran slightly faster with reduced intensity (please also compare with the loading control hybridized with a probe for GAPDH). (E) Western blot analysis of protein isolated from E10.5 wild-type (lanes 1 and 2) and mutant (lanes 3 and 4) embryos. Wild-type embryos displayed three bands of relative molecular mass 125×10^3, 110×10^3, and 80×10^3 which may represent isoforms of different sizes. The 125×10^3 band (arrow), which is the strongest band and may represent a full length isoform, is completely absent and the intensities of the smaller bands are significantly reduced in mutant embryos. Fifteen and 30 mg of proteins were loaded in lane 1 and 3, lanes 2 and 4, respectively.

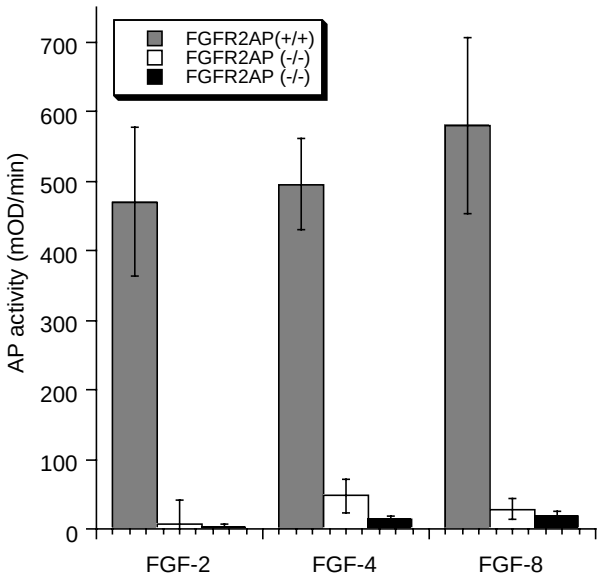

Fig. 2. FGF binding. Binding of wild-type and mutant FGFR2 to FGF immobilized on heparin sepharose. Soluble FGF receptor extracellular domain, fused to placental alkaline phosphatase (AP), was transiently expressed in COS-7 cells (see Materials and Methods). Equal amounts of wild-type (shaded) or mutant (clone 1, white; clone 2, black) FGFR2AP, normalized based on AP enzyme activity, were incubated with the indicated FGF. Bound receptor was quantified based on AP enzyme activity, as described in Materials and Methods.

mutants and control embryos (wild type or heterozygous) were similar in size (Fig. 3A and not shown). At E9.5, a portion of the *Fgfr2*$^{\Delta IgIII/\Delta IgIII}$ embryos (about 20%) were smaller (not shown). Mutants of this type were developmentally delayed at E10.5 (Fig. 3B), and some died at this stage. By E11.5, all the mutant embryos (n>30) were dead and partially or completely deteriorated (Fig. 3C,D). Histological analysis of E9.5 embryos in decidua revealed that the mutant placenta did not contain the allantoic component and failed to form a connection with the embryo (Fig. 3E,F). Apparently, the mutant placentas are non-functional, which is likely to account for the death of these embryos.

Failure of placental development in *Fgfr2*$^{\Delta IgIII/\Delta IgIII}$ embryos

A second defect, the failure of placental development, caused the death of the remaining two thirds of *Fgfr2*$^{\Delta IgIII/\Delta IgIII}$ embryos at E10-11.5. Unlike the first group of mutants, the chorion and allantois of these embryos were fused. At E9.5, both *Fgfr2*$^{\Delta IgIII/\Delta IgIII}$ and control embryos form a funnel-like structure at the chorioallantoic fusion junction (Fig. 4A,B). Mutant embryos have fewer trophoblast cells in the developing placenta (Fig. 4B). At E10.5, functional placentas were formed in the control embryos (Fig. 4E,G), however the mutant placentas developed abnormally (Fig. 4D,F,H,J,L) and displayed a variability in phenotype. In some cases, the fetal component of the mutant placentas failed to develop further and remained as funnel shaped structures resembling those of E9.5 (not shown). In other cases, the mutant allantoic mesoderm could undergo vascular differentiation to form placental blood vessels that were connected to an umbilical cord containing an artery and a vein (Fig. 4C). However, most blood vessels were found to be exposed at the surface of these placentas (Fig. 4D,J) due to a lack of labyrinthine trophoblast cells as revealed by histological sections (Fig. 4F,H). The placentas without labyrinthine portions may be partially functional because the mutant embryos with this structure survive slightly longer than other mutant embryos without chorioallantoic fusion (Fig. 6I and Fig. 7H for examples).

The placental defect was further analyzed using several lineage markers (Fig. 5). In situ hybridization with a probe for placental lactogen-1 (*pl-1*), which marks secondary giant cells (Guillemot et al., 1994; Fig. 5C), detected an expansion of the giant cell layer in mutant placentas (Fig. 5D). A direct counting of *pl-1*-expressing cells in 12 near-continuous sections from 2 mutant and 2 control placentas (three sections/placenta) revealed an average of 125 cells/section in mutant and 65 cells/section in control placentas. The second marker, *4311*, is expressed in the layer of spongiotrophoblasts in normal E9.5 placentas (Lescisin et al., 1988; Fig. 5E). Mutant placenta appearently contained the same number of spongiotrophoblasts (*4311*-expressing) cells, but these cells were somewhat disorganized compared to the *4311*-expressing cells in control embryos (Fig. 5E,F). The third marker used was *Mash-2* which is expressed in both spongiotrophoblast and labyrinthine

Table 1. Genotype and phenotype of offspring from intercrosses between *Fgfr2*$^{\Delta IgIII/+}$ mice

Age	Total decidua or embryos	Genotype			Abnormal embryos		
		+/+	*ΔIgIII/+*	*ΔIgIII/ΔIgIII*	No limb bud	Balloon allantois	Resorbed§
E9.5	104	24	55	22	22	9	3
E9.5*	35	8	17	6	6	2	4
E10.5	93	22	48	20	20	8	3
E10.5*	45	10	24	7	7	2	4
E11.5	95	25	44	18†	18†	7†	8
E12.5-14.5	108	28	45	5‡			30
P20-28	150	58	92	0			

*These embryos are in the 129 background. All others are in the background of 50% 129 and 50% Black Swiss. Mutants in both backgrounds showed similar phenotypes.

†Embryos were dead and, in most cases, partially resorbed.

‡Embryos were deteriorated and it could not be determined whether they had limb buds or not.

§Embryos were nearly or completerly resorbed and their genotype could not be reliably determined.

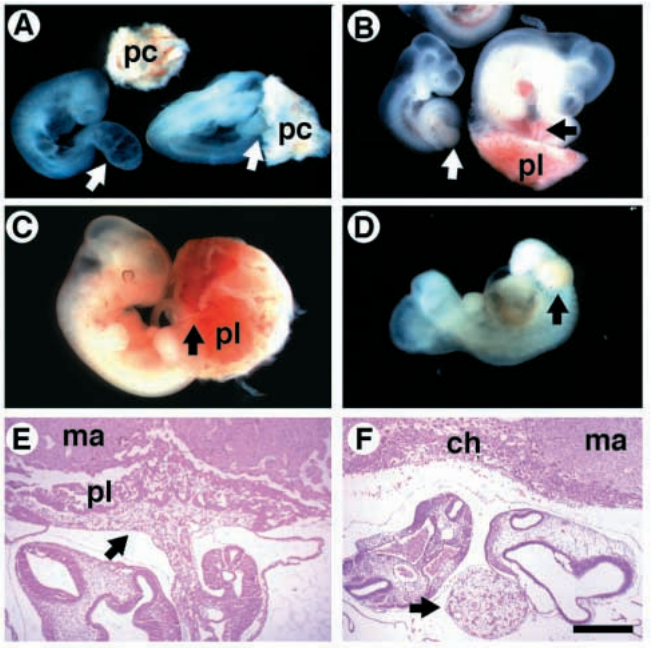

Fig. 3. A failure of chorioallantoic fusion in *Fgfr2*$^{\Delta IgIII/\Delta IgIII}$ embryos. (A,B) Absence of chorioallantoic fusion in *Fgfr2*$^{\Delta IgIII/\Delta IgIII}$ embryos at about E9.0 and E10.5 (left in A and B). The embryos on the right in A and B are wild-type or heterozygous controls. Arrows point to the allantois. (C,D) An E11.5 *Fgfr2*$^{\Delta IgIII/\Delta IgIII}$ embryo (D) and its littermate control (C). (E,F) Histological sections of E9.5 *Fgfr2*$^{\Delta IgIII/\Delta IgIII}$ (F) and control placentas (E). (ch) chorion; (ma) maternal portion of placenta; (pc) ectoplacenta cone; (pl) placenta. Bar shown in F can be used to measure all panels. It is 1.17 mm for A, 2.1 mm for B and C, 1 mm for D, 550 μm for E and F.

trophoblast in E9.5 control placentas (Fig. 5G). It has been shown previously that embryos carrying a null mutation of *Mash-2* lack spongiotrophoblasts and have a reduced labyrinthine area (Guillemot et al., 1994). In mutant placenta, *Mash-2* is expressed at a comparable level in spongiotrophoblasts, but its expression domain is smaller due to the absence of the adjacent labyrinthine layer (Fig. 5G,H). These data, combined with the histological analysis, revealed a specific block in the formation of labyrinthine part of the mutant placentas.

Early development of the labyrinthine placenta is characterized by rapid cellular proliferation. We next examined the proliferation of trophoblasts using an antibody against proliferating cell nuclear antigen (PCNA). Dramatic differences in the quantity of PCNA-expressing cells and/or expression levels of PCNA were detected by comparing placentas from *Fgfr2*$^{\Delta IgIII/\Delta IgIII}$ and control embryos. The majority (>70%) of placental trophoblasts were PCNA positive in controls (Fig. 4K), whereas PCNA-positive cells in all mutant placentas examined (n=7) were found to be not only sparse (<5%), but also of reduced intensity (Fig. 4L). Placentas were also examined for apoptosis. Less than 1% of the mesenchymal cells was found dead in both control and *Fgfr2*$^{\Delta IgIII/\Delta IgIII}$ placentas by TUNEL assay (not shown). These findings suggest that the failure of labyrinthine placenta development is caused by a block in proliferation of trophoblast cells, and not by an increase in cell death.

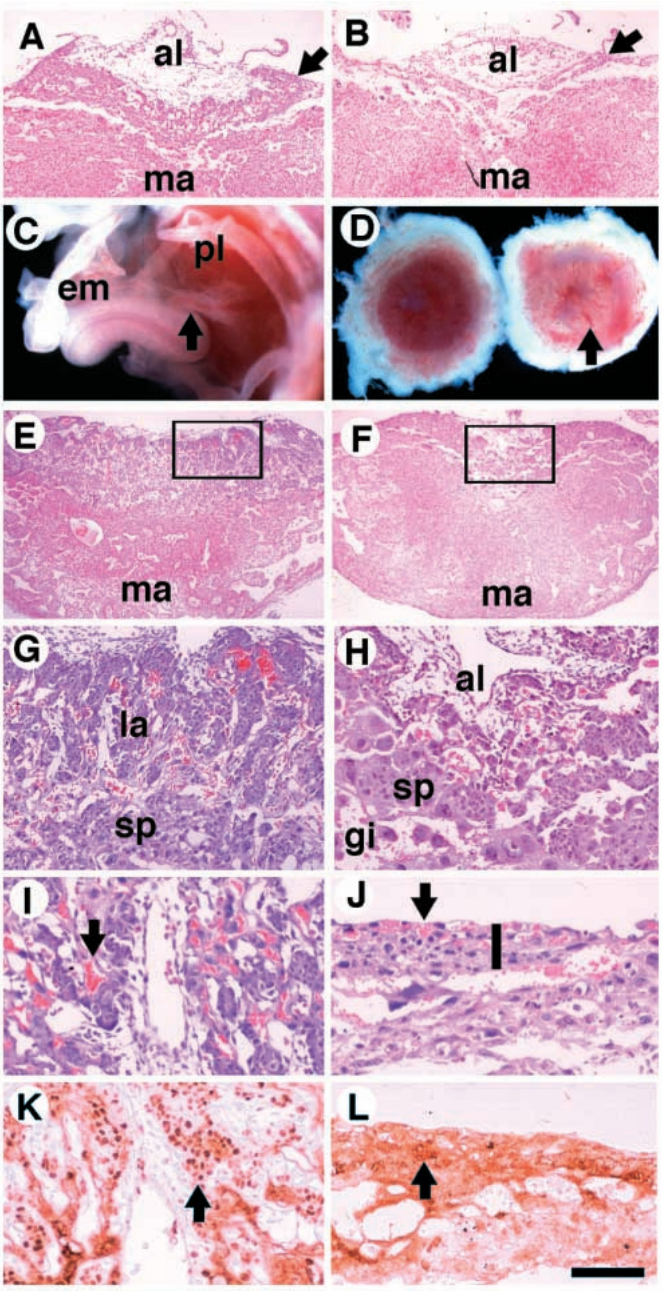

Fig. 4. A failure of functional placental formation in *Fgfr2*$^{\Delta IgIII/\Delta IgIII}$ embryos. (A,B) Fusion junctions (arrows) of chorion and allantois of E9.5 *Fgfr2*$^{\Delta IgIII/+}$ (A) and *Fgfr2*$^{\Delta IgIII/\Delta IgIII}$ (B) embryos. (C) An E10.5 *Fgfr2*$^{\Delta IgIII/\Delta IgIII}$ embryo possessing an umbilical cord with blood vessels (arrow). (D) Placentas isolated from a E10.5 *Fgfr2*$^{\Delta IgIII/\Delta IgIII}$ embryo (right) and its wild-type littermate (left). Arrow points to placenta blood vessels. (E-H) Transverse sections of E10.5 wild-type (E) and *Fgfr2*$^{\Delta IgIII/\Delta IgIII}$ (F) placentas. The boxed area in E and F are shown at a higher magnification in G and H, respectively. (I-J) Transverse sections of E10.5 wild-type (I) and *Fgfr2*$^{\Delta IgIII/\Delta IgIII}$ (J) placentas. The fetal portion of the wild-type placenta occupies the entire frame (I), whereas the mutant one is thinner (vertical line in J). Arrows point to blood vessels. (K-L) Immunohistochemical staining of placentas shown in I and J with an antibody to PCNA. Arrows point to PCNA-positive cells. (al) allantois; (em) embryo; (la) labyrinthine; (gi) secondary giant cells; (ma) maternal portion of placenta; (pl) placenta; (sp) spongiotrophoblasts. Bar: 550 μm in A,B,E and F, 900 μm in C, 1.6 mm in D, 110 μm in G-L.

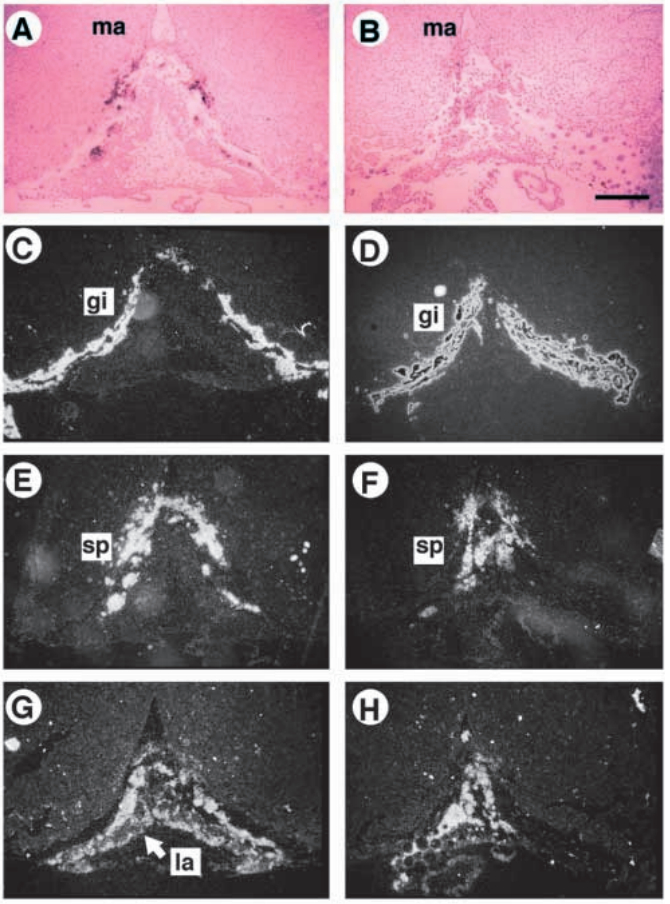

Fig. 5. Lineage-specific gene expression in *Fgfr2*$^{\Delta IgIII/\Delta IgIII}$ placentas. Near-adjacent sections from an E9.5 control placenta are shown in A, C, E and G, and an *Fgfr2*$^{\Delta IgIII/\Delta IgIII}$ placenta in B, D, F and H. (A,B) Bright-field images of the sections shown in E and F. All others are dark-field views. (C,D) Hybridization to the *pl-1* probe which marks secondary giant cells (gi). (E,F) Hybridization to a probe for 4311, a gene that is expressed in spongiotrophoblasts (sp) in E9.5 placentas. (G,H) Hybridization of *Mash-2*, a gene that is expressed in both spongiotrophoblasts and the labyrinthine trophoblasts (la) in E9.5 placentas. Bar: 500 μm in all panels.

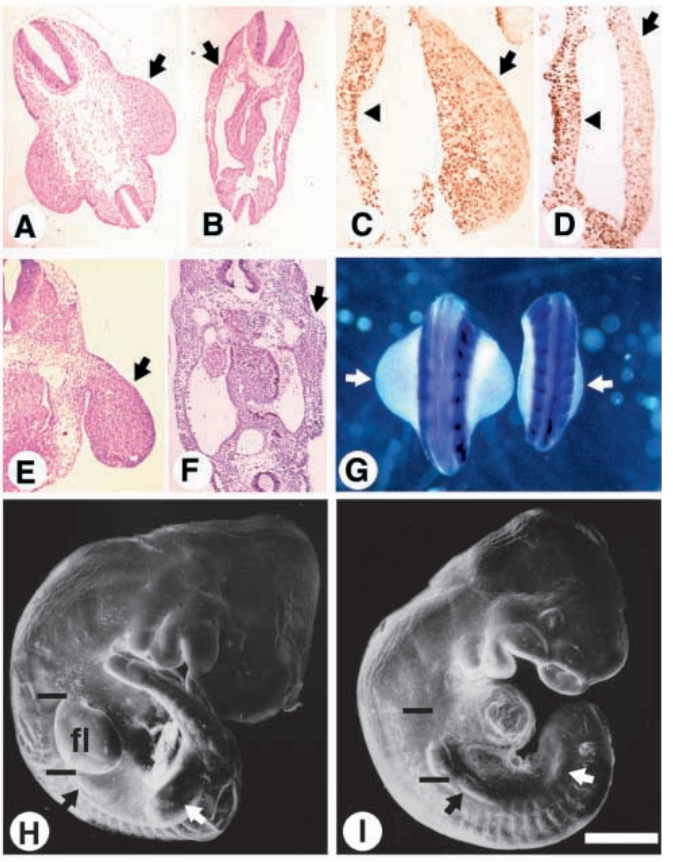

Fig. 6. Absence of limb buds in *Fgfr2*$^{\Delta IgIII/\Delta IgIII}$ embryos. (A,B) Histological sections of E9.5 embryos showing a control forelimb bud (arrow in A) and a mutant presumptive forelimb field (arrow in B). (C,D) Immunohistochemical staining of forelimb buds with PCNA antibody. The PCNA-positive cells in the mutant presumptive limb field (arrow in D) were very sparse compared with the control (arrow in C) whereas the PCNA staining in the control and mutant intermediate mesoderm (arrowheads) were comparable. (E,F) Sections of E10.75 embryos showing a control limb bud (arrow in E) and a mutant presumptive limb field (arrow in F). (G) Hindlimb buds of E10.75 embryos. The hindlimb field of the *Fgfr2*$^{\Delta IgIII/\Delta IgIII}$ embryo was significantly thickened (right arrow), however, it was much smaller than the control (left arrow). The samples were stained with *Mox-1* which marks all somites. The control embryo had 36 somites and the *Fgfr2*$^{\Delta IgIII/\Delta IgIII}$ embryo had 34 somites, respectively. (H,I) Scanning electron microscopy of E10.75 embryos. Both forelimb and hindlimb buds that are clearly visible in the control embryo (H) are absent in mutant embryo (I). The presumptive forelimb (fl) field is marked by two lines and the hindlimb field is indicated by white arrows. Notice a slight thickening of the side wall in the posterior portion of the mutant forelimb field (I). This feature was found in the majority of E10.5 *Fgfr2*$^{\Delta IgIII/\Delta IgIII}$ embryos. Black arrows points to the lateral ridge that is slightly bigger in mutants. Bar: 350 μm in A and B, 120 μm in C and D, 240 μm in E and F, 400 μm in G, and 700 μm in H and I.

The placental abnormality could result from fetal homozygosity for the *Fgfr2* mutation, maternal heterozygosity, or a combination of both, as the placenta contains both maternal and fetal cells. To examine this, blastocysts obtained from *Fgfr2*$^{\Delta IgIII/+}$ crosses were transferred to uteri of wild-type females. Examination of 5 E10.5 mutant placentas revealed identical phenotypes as described above. This observation indicates that the placental malformations result from FGFR2 deficiency in the fetal component.

Failure of limb induction in *Fgfr2*$^{\Delta IgIII/\Delta IgIII}$ embryos

A third abnormality seen in all *Fgfr2*$^{\Delta IgIII/\Delta IgIII}$ embryos is the failure to form limb buds. In normal development, forelimb initiation in mouse embryo begins around E9.25 with the continuous proliferation of lateral plate mesoderm cells, leading to the formation of a bulge under the ectoderm at the region lying between somites 8-12. Morphological and histological examinations of *Fgfr2*$^{\Delta IgIII/\Delta IgIII}$ embryos at stages between E9.25 (17 somites) and E10.75 (36 somites (n>50) indicated that the bulge was not formed (Fig. 6A,B,E,F,H,I). Immunohistochemistry of the presumptive limb field of mutant embryos revealed fewer PCNA-positive cells compared with their littermates (Fig. 6C,D), suggesting that the initial proliferation of mesenchyme is blocked in the

mutant limb field. Under a scanning electron microscope, the anterior portion of the presumptive forelimb field of E10.75 *Fgfr2*$^{\Delta IgIII/\Delta IgIII}$ embryos was completely flat although a slight thickening of the side wall was found in the posterior portion of the limb field (Fig. 6H,I). This suggests that loss of FGFR2 does not completely block the posterior limb field activity in some *Fgfr2*$^{\Delta IgIII/\Delta IgIII}$ embryos. However, histological sections that cross this region of E9.5-10.75 mutants did not reveal any structures that resemble the initiating limb buds (Fig. 6A,B,E,F). The hindlimb buds, which become visible at around E9.75 in normal embryos, were either absent (Fig. 6I) or very small compared to those of their littermate controls. One of the largest mutant 'hindlimb bud' and a control bud were included in Fig. 6G for comparison. Whole-mount in situ hybridization using markers for the zone of polarizing activity – Sonic hedgehog (*Shh*, Fig. 7I), and AER – *Fgf8* (Fig. 7G,H) and *Fgf4* (not shown), indicated that these structures were absent in the mutant presumptive forelimb and hindlimb fields because none of these markers were detected. Altogether, these data indicated that targeted deletion of Ig domain III of FGFR2 abolishes limb induction and generates limbless embryos.

Expression patterns of *Fgfr2, Fgf8* and *Fgf10* during early stages of limb induction

To understand how the FGFR2 deficiency leads to failure of limb bud initiation, markers of limb development were examined by in situ hybridization. Several members of the FGF family, including FGF1, FGF2, FGF4, FGF8 and FGF10, have been shown to promote complete limb formation in chick when ectopically supplied (Cohn et al., 1995; Crossley et al., 1996; Ohuchi et al., 1997). Although all these factors may potentially serve as endogenous limb inducers, *Fgf8* and *Fgf10* are the only two that are expressed at the right time and place (Crossley et al., 1996; Ohuchi et al., 1997). Ohuchi et al. (1997) demonstrated that FGF10 is the key mesenchymal factor, which initiates and maintains the outgrowth of the chick limb bud through interaction with FGF8. To understand the possible relationship between the *Fgfr2*, *Fgf8* and *Fgf10* genes during mouse limb initiation, their expression patterns were compared. In wild-type embryos, *Fgfr2* is transcribed in the lateral plate mesoderm by the onset of limb bud initiation (Orr-Urtreger et al., 1991). During the early stages of limb bud initiation, the *Fgfr2* transcripts were concentrated mainly in the surface ectoderm, and were expressed at a lower level in the adjacent mesenchyme (Fig. 7A). Expression of *Fgf10* in the presumptive limb field became visible in the lateral plate mesoderm around E9.0 (Fig 7B). It was initially expressed throughout the limb mesenchyme (Fig. 7C), and was later expressed preferentially in posterior and distal limb mesenchyme (Fig. 7F). Similar expression patterns were observed in hindlimb buds (see below). The *Fgf8* signals first became visible at the initiating limb bud ectoderm around E9.25 and were associated with the initial thickening of the lateral plate mesoderm (Fig. 7G). *Fgf8* expression was subsequently strongly induced in the ventral surface of the limb bud ectoderm before AER formation, and was expressed at very high levels along the entire length of the AER from the time that it first became morphologically distinct (about E10.0) until it regressed (about E12.5) (Fig. 7H and not shown). This indicated that although *Fgf8* and *Fgf10* expression patterns do not overlap with each other directly, both overlap the expression domain of *Fgfr2*. Interestingly, FGF8 has been shown to interact with the mesenchymally expressed spliced form of FGFR2 (BEK or FGFR2c), but not the epithelial spliced form (KGFR or FGFR2b) (MacArthur et al., 1995; Ornitz et al., 1996), whereas FGF10 only activates the FGFR2b (D.M.O. and A. Blunt, unpublished observation). This may suggest that both FGFs interact with different isoforms of FGFR2 in a paracrine fashion during limb bud initiation.

Fgf8 expression is absent in the presumptive limb field of *Fgfr2*$^{\Delta IgIII/\Delta IgIII}$ embryos

It was shown that FGF8 in the intermediate mesoderm induces its own expression in the surface ectoderm of the initiating limb bud (Crossley et al., 1996). Such an induction was suggested to be mediated by FGF10 (Ohuchi et al., 1997). The FGF8 in the limb ectoderm, in turn, acts on the underlying mesoderm to maintain *Fgf10* expression (Ohuchi et al., 1997). It is conceivable that the interactions between FGF8 and FGF10 are mediated by FGFR2 given the expression of *Fgfr2* both in the ectoderm and underlying mesenchyme. If this is the case, loss of FGFR2 should affect *Fgf8* induction in the limb bud ectoderm and *Fgf10* expression in the underlying mesoderm. To test this, we examined *Fgf10* and *Fgf8* expression patterns in the presumptive forelimb field of *Fgfr2*$^{\Delta IgIII/\Delta IgIII}$ embryos. Our data indicated that *Fgf10* transcripts were present in the presumptive forelimb field of all the E9.25-E9.75 mutant embryos examined (n=10). However, the intensity of the signals in the mutant embryos was significantly weaker than that seen in their wild-type littermates (Fig. 7C), and gradually diminished and disappeared in older mutant embryos (Fig. 7F). In contrast, *Fgf8* transcripts were absent in the presumptive limb field in all mutant embryos from E9.25 (Fig. 7G) through E10.75 (Fig. 7H) (n>30).

Expression of *Fgf8* and *Fgf10* was also examined in the hindlimb field of both normal and mutant embryos because significant thickening of the side wall was frequently observed in the mutant hindlimb fields (Fig 6G). In normal embryos, *Fgf10* expression becomes visible in the hindlimb field at E9.5 (not shown) and is strongly expressed at around E9.75, a time corresponding to hindlimb bud initiation (Fig. 7D). *Fgf10* was present in the mutant presumptive hindlimb field at a level lower than in wild type (Fig. 7E), and became even weaker in older embryos (Fig. 7F), and eventually disappeared (not shown). *Fgf8* transcripts were never detected in the mutant presumptive hindlimb field (n>15, not shown). Consistent with the hypothesis that FGF8 induces SHH (Grieshammer et al., 1996; Crossley et al., 1996). *Shh* transcript was never detected in the mutant limb presumptive field (Fig. 7I, n=12). Thus, loss of FGFR2 specifically blocks induction of *Fgf8* in the limb ectoderm and reduces *Fgf10* expression in the underlying mesoderm, suggesting the involvement of this receptor in a paracrine signaling loop between FGF8 and FGF10. Uncoupling of this epithelial-mesenchymal interaction loop may result in the failure of limb bud initiation.

Fgfr2$^{\Delta IgIII/\Delta IgIII}$ embryos have abnormal otic vesicles

Fgfr2 is also expressed in heart primordium, somites, neural tube, forebrain and midbrain of E8.5-10.5 embryos (Orr-

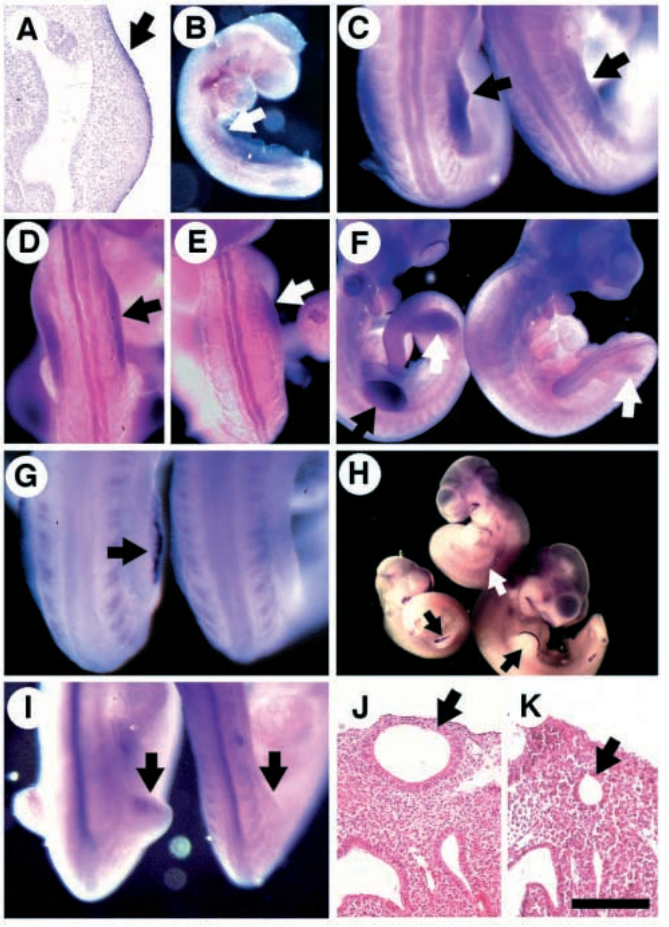

Fig. 7. Whole-mount analysis of *Fgfr2, Fgf8, Fgf10* and *Shh* in $Fgfr2^{\Delta IgIII/\Delta IgIII}$ and control embryos during limb bud initiation. (A) *Fgfr2* expression in wild-type E9.5 embryos. *Fgfr2* transcripts were concentrated in the ectoderm of limb buds and present at a lower level in the adjacent mesenchyme (arrow). (B-F) *Fgf10* expression. *Fgf10* transcripts were detected in the presumptive forelimb field at around E9.0 (arrow in B) and in mesenchyme of the initiating forelimb bud around E9.25-9.5 control embryos (left arrow in C). *Fgf10* expression is significantly down regulated in presumptive forelimb fields of $Fgfr2^{\Delta IgIII/\Delta IgIII}$ embryos (right arrow in C). (D) Initiating control hindlimb bud of approx. E10, showing *Fgf10* expression. (E) *Fgf10* is expressed in E10 mutant hindlimb field at a relatively lower level. (F) In E10.5 mutant embryos, *Fgf10* expression was significantly weaker (white arrows, which point out the hindlimb buds of the control (left) and mutant (right) respectively). Expression of *Fgf10* in mesenchyme was confirmed in tissue sections of forelimb or hindlimb buds (not shown). (G,H) *Fgf8* expression in E9.25 (G) and E10-10.75 (H) forelimb buds. Notice the absence of *Fgf8* expression in all mutant limb areas (right embryo in G is an 18-somite stage mutant, and the white arrow in H points to the limb area of a 36-somites mutant). (I) Whole-mount staining of E10 embryos with a riboprobe for Shh. Arrows point to ZPA that is absent in mutant presumptive limb field (right). (J,K) Otic vesicles of control (J) and mutant (K) embryos. Bar: 314 μm in A; 550 μm in B; 230 μm in C; 400 μm in D, E and I; 600 μm in F; 150 μm in G; 950 μm in H; 140 μm in J and K.

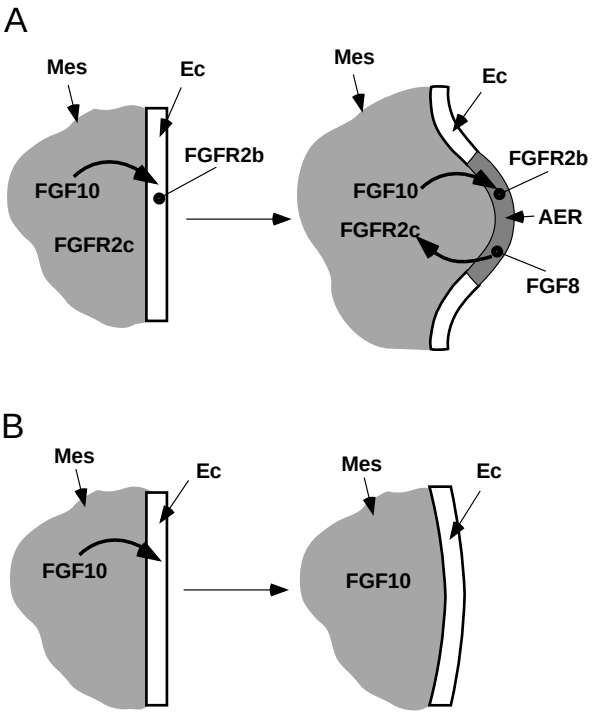

Fig. 8. A reciprocal signaling model showing the essential role of FGFR2 in epithelial-mesenchymal interactions during limb bud initiation. (A) Prior to limb bud initiation (before E9.25) in normal mouse embryos, *Fgf10* transcripts (dark shading) are detected in the mesenchyme (Mes) of the presumptive limb field. *Fgfr2b* and *Fgfr2c* are differentially expressed in the surface ectoderm (Ec, white bar) and the underlying mesenchyme, respectively. FGF10 induces *Fgf8* expression in the overlying surface ectoderm through the activation of the ectodermally expressed FGFR2b, and initiates outgrowth of the limb bud. Once it is induced, the FGF8 in the ectoderm interacts with the mesodermally expressed FGFR2c to maintain *Fgf10* expression and promote continuous proliferation of the underlying mesenchyme. Apical ectodermal ridge (AER) is subsequently induced by signals from proliferating mesenchyme. (B) In $Fgfr2^{\Delta IgIII/\Delta IgIII}$ embryos, expression of *Fgf10* in the mesenchyme can not induce *Fgf8* in the overlying ectoderm, suggesting an essential role of FGFR2 in this process. Without FGF8 signals from ectoderm, *Fgf10* expression is gradually diminished in the mutant mesoderm of the presumptive limb field. Uncoupling of this epithelial-mesenchymal signaling loop due to the loss of FGFR2 halts the proliferation mesenchymal cells at earliest stages of limb induction and generates limbless embryos.

Urtreger et al., 1993; Orr-Urtreger et al., 1991; and our unpublished observations). However, these regions were morphologically normal in $Fgfr2^{\Delta IgIII/\Delta IgIII}$ embryos (Figs 6G,H,I and 7F,H). Whole-mount in situ hybridization with several markers for these regions, including *Otx-2*, *Fgf8*, *en-1*, *Mox-1*, *Hoxb9* and *alpha-4* did not reveal obvious abnormalities except for the reduced sizes of the otic vesicles (Fig. 7F). In some mutant embryos, the otic vesicles were not visible and could only be seen in histological sections (Fig. 7K).

DISCUSSION

Mice carrying a targeted deletion of the Ig domain III of FGFR2 have been generated. We showed that mice heterozygous for the deletion were developmentally normal whereas homozygous embryos died at E10-11.5 due to a failure

in chorioallantoic fusion or in functional placental formation. We also showed that the deletion of Ig domain III of FGFR2 uncouples the reciprocal activation loop between FGF8 and FGF10 and generates embryos without limb buds. This finding provides direct genetic evidence that FGF/FGFR2 signals are required for vertebrate limb bud formation.

Mutant allele

We have shown that *Fgfr2*$^{\Delta IgIII/\Delta IgIII}$ mice die at E10-11.5 with multiple defects. This finding, however, seems contradictory to the observation that mice carrying a targeted deletion of the transmembrane and a portion of the TK domain of FGFR2 die at E4.5-5.5 (Arman, E., Chen, Y., Omin, M., Hafner-Krausz, R., and Lonai, P. Personal communication). Several attempts have been made to uncover the cause of this discrepancy. Genetic background frequently affects the penetrance of a mutation and has been reported to cause a dramatic difference in phenotypes of mice carrying a null mutation of the EGF receptor (Sibilia and Wagner, 1995; Threadgill et al., 1995). We, therefore, examined whether different backgrounds could affect the FGFR2 phenotype. Analysis of the FGFR2 mutation in a pure 129 background and a mixture of 129:Black Swiss did not reveal any apparent differences in *Fgfr2*$^{\Delta IgIII}$ phenotype, suggesting that the background differences cannot account for the above discrepancy. Next, we carefully examined transcription, translation and FGF binding of the *Fgfr2*$^{\Delta IgIII}$ allele at the RNA and protein levels. The results indicated that the deletion of exon 7-9 generated an in frame product that was transcribed at an average of about 20% of the wild-type level. Consistently, western blots detected a protein band with a reduced intensity and a smaller molecular mass. Thus, it is possible that the *Fgfr2*$^{\Delta IgIII}$ allele is not completely null and the protein lacking the Ig domain III still transmits a weak signal. If this is the case, it may account for the milder phenotype our *Fgfr2*$^{\Delta IgIII}$ mutants. However, in vitro assays have shown that both the Ig domain II and Ig domain III are required for high-affinity ligand binding (Zimmer et al., 1993). Loss of Ig domain III is predicted to reduce or completely abolish binding of the receptor to its ligands and, therefore, create a deficiency in FGFs/FGFR2 signaling. The failure of *Fgfr2*$^{\Delta IgIII}$ to interact with FGF2, FGF4 and FGF8 in in vitro binding analysis (Fig. 2) suggests that this may be the case. However, FGFR2 is a complex molecule that contains several other functional domains besides FGF binding. These include the acidic box and the CAM and heparin binding domains (Green et al., 1996; Mason, 1994). The potential functions of these domains are poorly characterized. Moreover, studies have shown that some cell adhesion molecules can signal through FGF receptor CAM binding domains (Green et al., 1996; Williams et al., 1994). We can not rule the possibility that the *Fgfr2*$^{\Delta IgIII}$ allele still retains functions that are independent of FGF binding, such as interaction with cell adhesion molecules. Precise understanding of the function of the *Fgfr2*$^{\Delta IgIII}$ mutant allele will require further study. Nevertheless, it is a loss-of-function mutation with respect to any FGF that requires the FGFR2 Ig domain III for signaling. Although the *Fgfr2*$^{\Delta IgIII}$ allele may not be a complete null, it has provided valuable information on the placental development and limb initiation processes that were not uncovered in mutant embryos completely lacking FGFR2.

FGFR2 is essential for placental formation

As revealed by the analysis of mutant embryos, the placenta is a site where the targeted mutation of FGFR2 exhibits a major impact. We showed that about 1/3 of *Fgfr2*$^{\Delta IgIII/\Delta IgIII}$ embryos have a failure in chorioallantois fusion, while the rest have abnormal placentas, indicating FGF/FGFR2 signals are essential for these processes. Chorioallantois fusion is the first step of a series of intrinsic events that sequentially occur during normal placental development. At about E10, the functional placenta forms and the embryonic and maternal circulation come into close contact, allowing the embryo to receive nutrients from the mother. The failure of chorioallantois fusion will undoubtedly result in the absence of a placenta, which is most likely a primary cause of death for the FGFR2 mutant embryos. The mechanism leading to failure in chorioallantoic fusion is not clear since many factors have been reported to interrupt the fusion process in rodents (reviewed by Cross et al., 1994). Notably, the failure in chorioallantois fusion in *Fgfr2*$^{\Delta IgIII/\Delta IgIII}$ embryos is similar to that caused by the targeted disruption of *Vcam-1* or *alpha-4* integrin (Gurtner et al., 1995; Kwee et al., 1995; Yang et al., 1995). Moreover, some VCAM-1 mutant embryos that are able to undergo chorioallantois fusion also die with a defect in the formation of the placental labyrinthine (Gurtner et al., 1995). FGFR2 is expressed in the chorion and allantois (Orr-Urtreger et al., 1991; and our unpublished observation) at the same time as *Vcam-1* and *alpha-4* integrin. It is likely that these factors interact with each other. We have compared the expression patterns of *Vcam-1* and *alpha-4* between the FGFR2 mutant and wild-type embryos, and could not find any obvious difference (not shown), ruling out the possibility that the defect in the *Fgfr2*$^{\Delta IgIII/\Delta IgIII}$ embryos is due to the loss or down regulation of the *Vcam-1* or *alpha-4* gene.

Early placental development at the post chorioallantoic fusion stage is characterized by a quick proliferation of trophoblast cells and an extensive vascularization in the labyrinthine portion of the placenta. Our data indicated that these processes depend upon FGF/FGFR2 signals since the mutant placentas exhibited poor vascularization and a virtually complete block in proliferation of trophoblast cells. Because the proliferation and vascularization are coupled events that are essential for labyrinthine placental development, the failure of normal placentation could be due to a block in either mitogenic or vascular differentiation signals, or the combination of the two. We found that the allantoic mesoderm could undergo angiogenesis to form placental blood vessels in over 50% of the mutant embryos. However, even this type of mutant embryos contained very few or no proliferative trophoblast cells as revealed by PCNA staining. These observations indicated that the primary defect in the FGFR2 embryo is the block in the trophoblast cell proliferation, leading to the failure in the labyrinthine portion of placenta. Thus, this study revealed an essential function of FGF/FGFR2 signaling as mitogenic stimuli for the cellular proliferation during both limb bud initiation and placentation. *Fgfr2*$^{\Delta IgIII/\Delta IgIII}$ embryos share some similarities with *Mash-2* homozygous embryos which also die due to a placental failure (Guillemot et al., 1994). Both mutants show an expansion in the layer of secondary giant cells and a defect in the labyrinthine portion of the placenta. However, the *Mash-2* mutants completely lack

spongiotrophoblasts whereas *Fgfr2*$^{\Delta IgIII/\Delta IgIII}$ embryos contain this type of cell. Our in situ hybridization indicated that *Mash-2* is expressed in the *Fgfr2*$^{\Delta IgIII/\Delta IgIII}$ spongiotrophoblasts at a level comparable to that of wild-type embryos (Fig. 5G,H). Thus, the relationship between FGFR2 and MASH2 is not clear and requires further study.

FGFR2 and limb development

Fibroblast growth factors have been considered as primary inductive signals in vertebrate limb induction because of their ability to replace the AER and to induce formation of a complete limb in chick (Cohn et al., 1995; Crossley et al., 1996; Fallon et al., 1994; Niswander and Martin, 1993; Niswander et al., 1993; Ohuchi et al., 1997; Vogel et al., 1996). However, these studies must be interpreted cautiously because they were done using either misexpression or an ectopic supply of FGFs, which raises the question of whether FGFs actually play the same role in vivo. It was suggested that FGF8 is an endogenous inducer of limb bud because it is expressed at the right time and place during limb bud initiation, while other FGFs may simply mimic FGF8 action (Crossley et al. 1996). However, recent studies in the chick limbless embryo showed that the initiation of the limb bud prior to the formation of AER can occur in the absence of FGF8 (Grieshammer et al., 1996; Ros et al., 1996), suggesting that FGF8 is not essential for initial outgrowth of the mesenchymal cells in the limb field. Moreover, targeted disruption of several FGFs in mice failed to provide any information that linked them to limb induction, because mice that carry a null mutation of each FGF either die at stages before limb induction or survive gestation without any limb abnormality (Feldman et al., 1995; Guo et al., 1996; Hebert et al., 1994; Mansour et al., 1993). Apparently, the analysis of the ligands involved in this critical process is complicated by both the potential functional redundancy of this 15-member gene family and the early lethality of some members. The present observation, that the targeted deletion of the Ig domain III domain of FGFR2 abolishes limb induction, provides direct genetic evidence that FGF signals are absolutely required in this process.

Limb initiation requires extensive epithelial-mesenchymal interactions (reviewed by Tabin, 1995). Previous studies suggested that, at the early stage prior to the AER formation, limb mesoderm contains signals necessary for the initiation of the limb buds (Ros et al., 1996; Stephens et al., 1989). Signals from ectoderm are responsible for the continuous proliferation of the underlying mesenchyme (Niswander and Martin 1993; Niswander et al. 1993; Fallon et al., 1994). FGF8 might be such a signal because of its expression at the right time and place (Crossley et al., 1996; Vogel et al., 1996). Specifically, Grieshammer et al. (1996) proposed that FGF8 signals are required for dorsal-ventral patterning and AER formation. However, it is not clear how FGF8, which is originally expressed in the intermediate mesoderm, carries out this function and induces its own expression in the surface ectoderm. A clue was provided by a recent study, which identified another member of FGF family, FGF10, as a mesenchymal factor involved in limb induction (Ohuchi et al., 1997). It was shown that *Fgf10* expression in the presumptive limb mesenchyme precedes *Fgf8* expression in the nascent apical ectoderm, and ectopic application of FGF10 to the chick embryonic flank induces *Fgf8* expression in the adjacent ectoderm and results in the formation of an additional complete limb (Ohuchi et al., 1997). Based on these observations, Ohuchi et al. (1997) postulated that the FGF10 could relay the FGF8 signal from the intermediate mesoderm and induce *Fgf8* expression in the overlying surface ectoderm. The expression of FGF8, in turn, acts on the underlying mesoderm to maintain FGF10 expression. Thus, the interaction between FGF8 and FGF10 mediates the epithelial-mesenchymal interaction required for limb induction. To identify the FGF receptors that are involved in this process, we have examined expression of all four known receptors (FGFR1-4) and found that *Fgfr1* and *Fgfr2* are the only receptors that showed significant expression at stages prior to AER formation. The absence of *Fgfr3* and *Fgfr4* suggests that these genes may not be responsible for limb bud initiation. This is consistent with our observation that mice deficient for both FGFR3 and FGFR4 have normal limb patterns (Weinstein, M. and Deng, C. unpublished data). *Fgfr1* expression is exclusively in the limb mesenchyme (Peters et al., 1992; and our own observation, not shown). Using chimeric embryos formed by FGFR1-deficient ES cells, we have previously shown that *Fgfr1* is not essential for limb initiation although it is important for the mesenchymal cell proliferation of limb buds (Deng et al., 1997). Two major isoforms of FGFR2 are expressed in the developing limb bud. The FGFR2IIIb is localized to the surface ectoderm, while the FGFR2IIIc isoform is expressed in the adjacent mesoderm (Orr-Urtreger et al., 1993). The differential expression of the two isoforms colocalizes with FGF10 in the mesenchyme and FGF8 in the ectoderm of the limb bud respectively, suggesting a direct interaction between this receptor and these ligands. Additional support comes from a recent observation that FGF8 promotes proliferation of cells that express FGFR2IIIc but not in cells that express FGFR2IIIb (MacArthur et al., 1995; Ornitz et al., 1996) whereas FGF10 was found only to activate FGFR2b (D.M.O. and A. Blunt, unpublished observation). These observations suggest that the two FGFs function in a paracrine fashion during limb induction. The finding that *Fgfr2*$^{\Delta IgIII/\Delta IgIII}$ embryos are limbless and failed to express *Fgf8* in mutant presumptive limb ectoderm provides genetic evidence for the involvement of FGFR2 in this process. We also found that *Fgf10* expression is gradually lost in the FGFR2 mutant presumptive limb mesoderm. Altogether, we propose that the two isoforms of FGFR2 differentially mediate signals of the two different FGFs during the early stages of limb bud initiation (Fig. 8). FGFR2b (KGFR), the ectodermally expressed isoform, is involved in the induction of FGF8 by FGF10 (inferred from findings that *Fgf8* transcripts were never detected in the FGFR2 mutant ectoderm (Fig. 7G,H) and that FGF10 only can activate FGFR2b). FGF8, in turn, interacts with FGFR2c (BEK), the mesenchymally expressed isoform, to maintain expression of FGF10, to induce SHH, and to promote the continuous outgrowth of the underlying mesoderm cells (inferred from findings that *Fgf10* expression is gradually diminished in the FGFR2 mutant presumptive limb mesoderm (Fig 7C-F) and FGF8 specifically activates FGFR2c; MacArthur et al., 1995; Ornitz et al., 1996). Loss of FGFR2 disrupts this reciprocal activation loop and results in the failure of limb induction.

We thank C. Chiang for *Shh*, C. MacArther for *Fgf8*, C. V. E. Wright for *Mox-1* and J. Rossant for *4311*, *pl-1* and *Mash-2* probes.

We are grateful to V. Knezevic, S. Mackem and J. M. Gotay for helpful discussions and critical reading of the manuscript. We also thank B. Swain for assistance with the scanning electronic microscope. D. M. O. is supported by grant CA60673 from the NCI. M. N. is supported by a Howard Hughes physician scientist award.

REFERENCES

Amaya, E., Musci, T. J. and Kirschner, M. W. (1991). Expression of a dominant negative mutant of the FGF receptor disrupts mesoderm formation in Xenopus embryos. *Cell* **66,** 257-270.

Basilico, C. and Moscatelli, D. (1992). The FGF family of growth factors and oncogenes. *Adv. Cancer Re.s* **59,** 115-165.

Beiman, M., Shilo, B. Z. and Volk, T. (1996). Heartless, a Drosophila FGF receptor homolog, is essential for cell migration and establishment of several mesodermal lineages. *Genes Dev.* **10,** 2993-3002.

Candia, A. F., Hu, J., Crosby, J., Lalley, P. A., Noden, D., Nadeau, J. H. and Wright, C. V. (1992). Mox-1 and Mox-2 define a novel homeobox gene subfamily and are differentially expressed during early mesodermal patterning in mouse embryos. *Development* **116,** 1123-1136.

Capecchi, M. R. (1989). Altering the genome by homologous recombination. [Review]. *Science* **244,** 1288-1292.

Chellaiah, A. T., McEwen, D. G., Werner, S., Xu, J. and Ornitz, D. M. (1994). Fibroblast growth factor receptor (FGFR) 3. Alternative splicing in immunoglobulin-like domain III creates a receptor highly specific for acidic FGF/FGF-1. *J. Biol. Chem.* **269,** 11620-11627.

Chiang, C., Litingtung, Y., Lee, E., Young, K. E., Corden, J. L., Westphal, H. and Beachy, P. A. (1996). Cyclopia and defective axial patterning in mice lacking Sonic hedgehog gene function. *Nature* **383,** 407-413.

Ciruna, B. G., Schwartz, L., Harpal, K., Yamaguchi, T. P. and Rossant, J. (1997). Chimeric analysis of fibroblast growth factor receptor-1 (Fgfr1) function: a role for FGFR1 in morphogenetic movement through the primitive streak. *Development* **124,** 2829-2841.

Cohn, M. J., Izpisua-Belmonte, J. C., Abud, H., Heath, J. K. and Tickle, C. (1995). Fibroblast growth factors induce additional limb development from the flank of chick embryos. *Cell* **80,** 739-746.

Colvin, J. S., Bohne, B. A., Harding, G. W., McEwen, D. G. and Ornitz, D. M. (1996). Skeletal overgrowth and deafness in mice lacking fibroblast growth factor receptor 3. *Nat. Genet.* **12,** 390-397.

Cross, J. C., Werb, Z. and Fisher, S. J. (1994). Implantation and the placenta: key pieces of the development puzzle. *Science* **266,** 1508-1518.

Crossley, P. H. and Martin, G. R. (1995). The mouse *Fgf8* gene encodes a family of polypeptides and is expressed in regions that direct outgrowth and patterning in the developing embryo. *Development* **121,** 439-451.

Crossley, P. H., Minowada, G., MacArthur, C. A. and Martin, G. R. (1996). Roles for FGF8 in the induction, initiation, and maintenance of chick limb development. *Cell* **84,** 127-136.

Deng, C., Bedford, M., Li, C., Xu, X., Yang, X., Dunmore, J. and Leder, P. (1997). Fibroblast growth factor receptor-1 (FGFR-1) is essential for normal neural tube and limb development. *Dev. Biol.* **185,** 42-54.

Deng, C., Wynshaw-Boris, A., Zhou, F., Kuo, A. and Leder, P. (1996). Fibroblast growth factor receptor 3 is a negative regulator of bone growth. *Cell* **84,** 911-21.

Deng, C. X., Wynshaw-Boris, A., Shen, M. M., Daugherty, C., Ornitz, D. M. and Leder, P. (1994). Murine FGFR-1 is required for early postimplantation growth and axial organization. *Genes Dev.* **8,** 3045-3057.

DeVore, D. L., Horvitz, H. R. and Stern, M. J. (1995). An FGF receptor signaling pathway is required for the normal cell migrations of the sex myoblasts in C. elegans hermaphrodites. *Cell* **83,** 611-620.

Fallon, J. F., Lopez, A., Ros, M. A., Savage, M. P., Olwin, B. B. and Simandl, B. K. (1994). FGF-2: apical ectodermal ridge growth signal for chick limb development. *Science* **264,** 104-107.

Feldman, B., Poueymirou, W., Papaioannou, V. E., DeChiara, T. M. and Goldfarb, M. (1995). Requirement of FGF-4 for postimplantation mouse development. *Science* **267,** 246-249.

Gisselbrecht, S., Skeath, J. B., Doe, C. Q. and Michelson, A. M. (1996). Heartless encodes a fibroblast growth factor receptor (DFR1/DFGF-R2) involved in the directional migration of early mesodermal cells in the Drosophila embryo. *Genes Dev.* **10,** 3003-17.

Givol, D. and Yayon, A. (1992). Complexity of FGF receptors: genetic basis for structural diversity and functional specificity. *FASEB J.* **6,** 3362-3369.

Gray, T. E., Eisenstein, M., Shimon, T., Givol, D. and Yayon, A. (1995). Molecular modeling based mutagenesis defines ligand binding and specificity determining regions of fibroblast growth factor receptors. *Biochemistry* **34,** 10325-10333.

Green, P. J., Walsh, F. S. and Doherty, P. (1996). Promiscuity of fibroblast growth factor receptors. *BioEssays* **18,** 639-646.

Grieshammer, U., Minowada, G., Pisenti, J. M., Abbott, U. K. and Martin, G. R. (1996). The chick *limbless* mutation causes abnormalities in limb bud dorsal-ventral patterning: implications for the mechanism of apical ridge formation. *Development* **122,** 3851-3861.

Guillemot, F., Nagy, A., Auerbach, A., Rossant, J. and Joyner, A. L. (1994). Essential role of Mash-2 in extraembryonic development. *Nature* **371,** 333-336.

Guo, L., Degenstein, L. and Fuchs, E. (1996). Keratinocyte growth factor is required for hair development but not for wound healing. *Genes Dev.* **10,** 165-175.

Gurtner, G. C., Davis, V., Li, H., McCoy, M. J., Sharpe, A. and Cybulsky, M. I. (1995). Targeted disruption of the murine VCAM1 gene: essential role of VCAM-1 in chorioallantoic fusion and placentation. *Genes Dev.* **9,** 1-14.

Hebert, J. M., Rosenquist, T., Gotz, J. and Martin, G. R. (1994). FGF5 as a regulator of the hair growth cycle: evidence from targeted and spontaneous mutations. *Cell* **78,** 1017-1025.

Heikinheimo, M., Lawshe, A., Shackleford, G. M., Wilson, D. B. and MacArthur, C. A. (1994). Fgf-8 expression in the post-gastrulation mouse suggests roles in the development of the fact, limbs and central nervous system. *Mech. Dev.* **48**, 129-138.

Johnson, D. E. and Williams, L. T. (1993). Structural and functional diversity in the FGF receptor multigene family. *Adv. Cancer Res*. **60,** 1-41.

Kwee, L., Baldwin, H. S., Shen, H. M., Stewart, C. L., Buck, C., Buck, C. A. and Labow, M. A. (1995). Defective development of the embryonic and extraembryonic circulatory systems in vascular cell adhesion molecule (VCAM-1) deficient mice. *Development* **121,** 489-503.

Laufer, E., Nelson, C. E., Johnson, R. L., Morgan, B. A. and Tabin, C. (1994). Sonic hedgehog and Fgf-4 act through a signaling cascade and feedback loop to integrate growth and patterning of the developing limb bud. *Cell* **79,** 993-1003.

Lescisin, K. R., Varmuza, S. and Rossant, J. (1988). Isolation and characterization of a novel trophoblast-specific cDNA in the mouse. *Genes Dev.* **2,** 1639-1646.

Li, E., Bestor, T. H. and Jaenisch, R. (1992). Targeted mutation of the DNA methyltransferase gene results in embryonic lethality. *Cell* **69,** 915-926.

MacArthur, C. A., Lawshe, A., Xu, J., Santos-Ocampo, S., Heikinheimo, M., Chellaiah, A. T. and Ornitz, D. M. (1995). FGF-8 isoforms activate receptor splice forms that are expressed in mesenchymal regions of mouse development. *Development* **121,** 3603-3613.

Mahmood, R., Bresnick, J., Hornbruch, A., Mahony, C., Morton, N., Colquhoun, K., Martin, P., Lumsden, A., Dickson, C. and Mason, I. (1995). A role for FGF-8 in the initiation and maintenance of vertebrate limb bud outgrowth. *Curr. Biol*. **5,** 797-806.

Mansour, S. L., Goddard, J. M. and Capecchi, M. R. (1993). Mice homozygous for a targeted disruption of the proto-oncogene int-2 have developmental defects in the tail and inner ear. *Development* **117,** 13-28.

Mason, I. (1994). Cell signalling. Do adhesion molecules signal via FGF receptors? *Curr. Biol.* **4,** 1158-1161.

McWhirter, J. R., Goulding, M., Weiner, J. A., Chun, J. and Murre, C. (1997). A novel fibroblast growth factor gene expressed in the developing nervous system is a downstream target of the chimeric homeodomain oncoprotein E2A-Pbx1. *Development* **124,** 3221-3232.

Muenke, M. and Schell, U. (1995). Fibroblast-growth-factor receptor mutations in human skeletal disorders. *Trends Genet*. **11,** 308-313.

Mulvihill, J. J. (1995). Craniofacial syndromes: no such thing as a single gene disease [published erratum appears in *Nat. Genet.* (1995) **9**(4), 451]. *Nat. Genet.* **9,** 101-103.

Niswander, L., Jeffrey, S., Martin, G. R. and Tickle, C. (1994). A positive feedback loop coordinates growth and patterning in the vertebrate limb [see comments]. *Nature* **371,** 609-612.

Niswander, L. and Martin, G. R. (1993). FGF-4 and BMP-2 have opposite effects on limb growth. *Nature* **361,** 68-71.

Niswander, L., Tickle, C., Vogel, A., Booth, I. and Martin, G. R. (1993). FGF-4 replaces the apical ectodermal ridge and directs outgrowth and patterning of the limb. *Cell* **75,** 579-587.

Ohuchi, H., Nakagawa, T., Yamamoto, A., Araga, A., Ohata, T., Ishimaru, Y., Yoshioka, H., Kuwana, T., Nohno, T., Yamasaki, M., Itoh, N. and Noji, S. (1997). The mesenchymal factor, FGF10, initiates and maintains the outgrowth of the chick limb bud through interaction with FGF8, an apical ectodermal factor. *Development* **124,** 2235-2244.

Ornitz, D. M., Xu, J., Colvin, J. S., McEwen, D. G., MacArthur, C. A., Coulier, F., Gao, G. and Goldfarb, M. (1996). Receptor specificity of the fibroblast growth factor family. *J. Biol. Chem.* **271,** 15292-15297.

Orr-Urtreger, A., Bedford, M. T., Burakova, T., Arman, E., Zimmer, Y., Yayon, A., Givol, D. and Lonai, P. (1993). Developmental localization of the splicing alternatives of fibroblast growth factor receptor-2 (FGFR2). *Dev. Biol.* **158,** 475-486.

Orr-Urtreger, A., Givol, D., Yayon, A., Yarden, Y. and Lonai, P. (1991). Developmental expression of two murine fibroblast growth factor receptors, flg and bek. *Development* **113,** 1419-1434.

Peters, K., Ornitz, D., Werner, S. and Williams, L. (1993). Unique expression pattern of the FGF receptor 3 gene during mouse organogenesis. *Dev. Biol.* **155,** 423-430.

Peters, K., Werner, S., Liao, X., Wert, S., Whitsett, J. and Williams, L. (1994). Targeted expression of a dominant negative FGF receptor blocks branching morphogenesis and epithelial differentiation of the mouse lung. *EMBO J.* **13,** 3296-301.

Peters, K. G., Werner, S., Chen, G. and Williams, L. T. (1992). Two FGF receptor genes are differentially expressed in epithelial and mesenchymal tissues during limb formation and organogenesis in the mouse. *Development* **114,** 233-243.

Przylepa, K. A., Paznekas, W., Zhang, M., Golabi, M., Bias, W., Bamshad, M. J., Carey, J. C., Hall, B. D., Stevenson, R., Orlow, S., Cohen, M. M., Jr. and Jabs, E. W. (1996). Fibroblast growth factor receptor 2 mutations in Beare-Stevenson cutis gyrata syndrome. *Nat. Genet.* **13,** 492-494.

Reichman-Fried, M., Dickson, B., Hafen, E. and Shilo, B. Z. (1994). Elucidation of the role of breathless, a Drosophila FGF receptor homolog, in tracheal cell migration. *Genes Dev.* **8,** 428-439.

Reichman-Fried, M. and Shilo, B. Z. (1995). Breathless, a Drosophila FGF receptor homolog, is required for the onset of tracheal cell migration and tracheole formation. *Mech. Dev.* **52,** 265-273.

Riddle, R. D., Johnson, R. L., Laufer, E. and Tabin, C. (1993). Sonic-hedgehog mediates the polarizing activity of the zpa. *Cell* **75,** 1401-1416.

Ros, M. A., Lopez-Martinez, A., Simandl, B. K., Rodriguez, C., Izpisua Belmonte, J. C., Dahn, R. and Fallon, J. F. (1996). The limb field mesoderm determines initial limb bud anteroposterior asymmetry and budding independent of sonic hedgehog or apical ectodermal gene expressions. *Development* **122,** 2319-2330.

Savage, M. P. and Fallon, J. F. (1995). FGF-2 mRNA and its antisense message are expressed in a developmentally specific manner in the chick limb bud and mesonephros. *Dev. Dyn.* **202,** 343-353.

Sibilia, M. and Wagner, E. F. (1995). Strain-dependent epithelial defects in mice lacking the EGF receptor [published erratum appears in Science (1995) No, 5226, page 909. *Science* **269,** 234-238.

Smallwood, P. M., Munoz-Sanjuan, I., Tong, P., Macke, J. P., Hendry, S. H., Gilbert, D. J., Copeland, N. G., Jenkins, N. A. and Nathans, J. (1996). Fibroblast growth factor (FGF) homologous factors: new members of the FGF family implicated in nervous system development. *Proc. Natl. Acad. Sci. USA* **93,** 9850-9857.

Stark, K. L., McMahon, J. A. and McMahon, A. P. (1991). FGFR-4, a new member of the fibroblast growth factor receptor family, expressed in the definitive endoderm and skeletal muscle lineages of the mouse. *Development* **113,** 641-651.

Stephens, T. D., Beier, R. L., Bringhurst, D. C., Hiatt, S. R., Prestridge, M., Pugmire, D. E. and Willis, H. J. (1989). Limbness in the early chick embryo lateral plate. *Dev. Biol.* **133,** 1-7.

Tabin, C. (1995). The initiation of the limb bud: growth factors, Hox genes, and retinoids. *Cell* **80,** 671-674.

Threadgill, D. W., Dlugosz, A. A., Hansen, L. A., Tennenbaum, T., Lichti, U., Yee, D., LaMantia, C., Mourton, T., Herrup, K., Harris, R. C. and et al. (1995). Targeted disruption of mouse EGF receptor: effect of genetic background on mutant phenotype. *Science* **269,** 230-234.

Tybulewicz, V. L., Crawford, C. E., Jackson, P. K., Bronson, R. T. and Mulligan, R. C. (1991). Neonatal lethality and lymphopenia in mice with a homozygous disruption of the c-abl proto-oncogene. *Cell* **65,** 1153-1163.

Verdier, A. S., Mattei, M. G., Lovec, H., Hartung, H., Goldfarb, M., Birnbaum, D. and Coulier, F. (1997). Chromosomal mapping of two novel human FGF genes, FGF11 and FGF12. *Genomics* **40,** 151-154.

Vogel, A., Rodriguez, C. and Izpisua-Belmonte, J. C. (1996). Involvement of FGF-8 in initiation, outgrowth and patterning of the vertebrate limb. *Development* **122,** 1737-1750.

Werner, S., Weinberg, W., Liao, X., Peters, K. G., Blessing, M., Yuspa, S. H., Weiner, R. L. and Williams, L. T. (1993). Targeted expression of a dominant-negative FGF receptor mutant in the epidermis of transgenic mice reveals a role of FGF in keratinocyte organization and differentiation. *EMBO J.* **12,** 2635-2643.

Williams, E. J., Furness, J., Walsh, F. S. and Doherty, P. (1994). Activation of the FGF receptor underlies neurite outgrowth stimulated by L1, N-CAM, and N-cadherin. *Neuron* **13,** 583-594.

Yamaguchi, T. P., Conlon, R. A. and Rossant, J. (1992). Expression of the fibroblast growth factor receptor FGFR-1/flg during gastrulation and segmentation in the mouse embryo. *Developmental Biology* **152,** 75-88.

Yamaguchi, T. P., Harpal, K., Henkemeyer, M. and Rossant, J. (1994). fgfr-1 is required for embryonic growth and mesodermal patterning during mouse gastrulation. *Genes Dev* **8,** 3032-3044.

Yamasaki, M., Miyake, A., Tagashira, S. and Itoh, N. (1996). Structure and expression of the rat mRNA encoding a novel member of the fibroblast growth factor family. *J. Biol. Chem.* **271,** 15918-15921.

Yang, J. T., Rayburn, H. and Hynes, R. O. (1995). Cell adhesion events mediated by alpha 4 integrins are essential in placental and cardiac development. *Development* **121,** 549-560.

Yayon, A., Zimmer, Y., Shen, G. H., Avivi, A., Yarden, Y. and Givol, D. (1992). A confined variable region confers ligand specificity on fibroblast growth factor receptors: implications for the origin of the immunoglobulin fold. *EMBO J.* **11,** 1885-1890.

Zimmer, Y., Givol, D. and Yayon, A. (1993). Multiple structural elements determine ligand binding of fibroblast growth factor receptors. Evidence that both Ig domain 2 and 3 define receptor specificity. *J. Biol. Chem.* **268,** 7899-7903.